Journal of Power Sources 196 (2011) 1555–1560

Contents lists available at ScienceDirect

Journal of Power Sources

journal homepage: www.elsevier.com/locate/jpowsour

Lead-acid batteries in micro-hybrid applications. Part II. Test proposal

S. Schaeck[a,*], A.O. Stoermer[a], J. Albers[b], D. Weirather-Koestner[c], H. Kabza[d]

[a] BMW Group, 80788 München, Germany
[b] Johnson Controls Power Solutions EMEA, 30419 Hannover, Germany
[c] ZSW Ulm, 89081 Ulm, Germany
[d] Universität Ulm, Institut für Energiewandlung und -speicherung, 89081 Ulm, Germany

ARTICLE INFO

Article history:
Received 5 July 2010
Received in revised form 24 August 2010
Accepted 25 August 2010
Available online 29 September 2010

Keywords:
Valve-regulated lead-acid battery (VRLA)
Micro-hybrid electric vehicle
Accelerated aging test
Dynamic charge acceptance

ABSTRACT

In the first part of this work [1] selected key parameters for applying lead-acid (LA) batteries in micro-hybrid power systems (MHPS) were investigated. Main results are integrated in an accelerated, comprehensive test proposal presented here. The test proposal aims at a realistic representation of the pSoC operation regime, which is described in Refs. [1,6]. The test is designed to be sensitive with respect to dynamic charge acceptance (DCA) at partially discharged state (critical for regenerative braking) and the internal resistance at high-rate discharge (critical for idling stop applications). First results are presented for up-to-date valve-regulated LA batteries with absorbent glass mat (AGM) separators. The batteries are close to the limits of the first proposal of pass/fail-criteria. Also flooded batteries were tested; the first out of ten units failed already.

1. Introduction

In part I of this publication main key parameters for the application of lead-acid (LA) batteries in micro-hybrid power systems (MHPS) were introduced [1]. Dynamic charge acceptance (DCA), overcharge robustness, warm crank performance and robustness against deep discharges were investigated. Several experiments were presented in order to investigate cause and effect. However, in the discussion these key parameters were considered separate from each other. In real-life vehicle operation a mixture of the presented phenomena affects battery degradation. Therefore, preferably comprehensive test procedures are desired for releasing LA batteries for MHPS. Such test procedures should reflect the application in the field as realistically as possible. Furthermore, such test procedures are expected to be accelerated, i.e. the battery cycle-life should ideally be covered within several weeks. Up-to-date battery test procedures in the automotive industry have their origin in the application of maintenance-free flooded LA batteries in the conventional power system (CPS) and can be found e.g. in the European and German standard DIN EN 50342-1 [2] and diverse other national standards. The German car makers and battery suppliers are working out proposals for new standards and regulations for automotive batteries within the working group AK 371.04 of the 'Deutsche Elektrotechnische Kommission' (DKE) [3]. Sophisticated electric cycling tests in order to characterize and approve LA batteries for OEM application were designed within this framework. Examples for such up-to-date homologation tests are the '17.5% DoD (depth of discharge) test', the '50% DoD test' or diverse particular lifetime tests as specified for example in the BMW Group Standard for SLI batteries [4] or in corresponding specifications by other OEMs.

Each of these tests is supposed to cover specific battery degradation phenomena. For example, the '17.5%' DoD test is especially appropriate for verifying battery cyclability in terms of softening and adhesion of the positive active mass (PAM). Another example is the 'corrosion test' for examination of growth and corrosion of the positive grid.

There are a few drawbacks of these tests concerning LA batteries in MHPS. Firstly, the tests are not quite representative for vehicle operation. Of course, none of the accelerated tests is realistic, however, not even subsections of the tests would occur in accordance with real-life-application. Nevertheless, the tests are suitable for the release of LA batteries as they are widely accepted in the battery community and give insight into design aspects and durability and endurance features. Secondly, none of the test reflects the typical load profile in micro-hybrid applications at pSoC. Hence, a test proposal is given in the next section. First results are presented, too.

2. Test proposal

The presented test will be termed 'micro-cycling test' (MCT) in the following. It is designed as an accelerated test for reproducing the specific operational features of LA batteries in the MHPS. According to Ref. [1] it aims at the most critical parameters of LA

* Corresponding author. Tel.: +49 89 382 78653; fax: +49 89 382 42827.
E-mail addresses: stefan.schaeck@bmw.de, stefan.schaeck@gmx.de (S. Schaeck).

0378-7753/$ – see front matter © 2010 Elsevier B.V. All rights reserved.
doi:10.1016/j.jpowsour.2010.08.079

Table 1
Procedure of the micro-cycling test proposal. The main design feature of the test is determined by the steps 5–16 forming one cycle iteration. Here, the theoretical amount of charge offered is sufficient for a positive charge balance (approved up to CF = 1.1 and for brand-new batteries) if battery DCA is sufficiently high. This is illustrated by Fig. 1 on the right where the SoC at the end of one cycle iteration is higher than the SoC at the beginning. If battery DCA decreases or the charge factor becomes CF ≥ 1.1, the SoC effectively shrinks.

Micro-cycling test: $T = 25\,^{\circ}C$					
Step 1				Type	Parameters
1				Discharge	$I = I_{20}$ $U = 10.5$ V
2				IU-Charge	$U = 14.8$ V $I = I_5$ $t = 24$ h
3	×10			Break	$t = 6$ h
4	unit			Discharge	SoC = 80% C_{20} O_m (acc. to step 1 or 20)
5		×50		Break	$t = 1$ h
6		cycle		Warm crank (optional)	$I = 400$ A $t = 1$ s
7			×6 block	Discharge	$I = 50$ A $t = 50$ s
8				IU-Charge	$U = 14.8$ V $t = 10$ s
9				Break	$t = 1$ h
10				Warm crank (optional)	$I = 400$ A $t = 1$ s
11			×47	Discharge	$I = 50$ A $t = 50$ s
12				IU-Charge	$U = 14.8$ V $t = 10$ s
13				Break	$t = 1$ h
14				Warm crank (optional)	$I = 400$ A $t = 1$ s
15			×6	Discharge	$I = 50$ A $t = 50$ s
16				IU-Charge	$U = 14.8$ V $t = 10$ s
17				Break	$t = 4$ h
18				Discharge	$I = I_{20}$ $U = 14.5$ V
19				IU-Charge	$U = 14.8$ V $I = I_5$ $I = 24$ A
20				Discharge	$I = I_{20}$ $U = 10.5$ V
21				IU-Charge	$U = 14.8$ V $I = I_5$ $I = 24$ A

batteries for application with BER, i.e. dynamic charge acceptance (DCA), and for ASSF, i.e. internal resistance R_i. The test is based on a micro-cycling template, which was originally developed by Albers et al. [5]. In order to observe additional effects in the field, the MCT was adapted by BMW to be closer to real-life conditions. This test profile is shown in Table 1 and graphically illustrated in Fig. 1. The MCT is performed at room temperature and the SoC is adjusted to 80% (step 4 in Table 1). Following a break of 1 h a high-rate discharge simulates an ASSF warm crank (step 6). After that, six micro cycles with negative charge balance are performed. This is illustrated in Fig. 1 and termed as micro-cycling block in the following. The amount of discharge is 6×0.694 Ah (step 7) whereas the amount of charge depends on battery DCA. The maximum possible amount of charge during 'boost charging' for 10 s is 0.138 Ah. (The maximum charge current is limited to 50 A. This enables to perform the test also with standard 12 V test equipment if the warm cranks (steps 6, 10, 14) are skipped.) Therefore, even if DCA remains permanently at the upper level of 50 A during step 8, the balanced DoD is −3.7% after the 6-fold micro-cycle block (if the test is performed with a 90 Ah battery). The worst case is −4.82% DoD. Then, a vehicle rest time of 1 h is performed (step 9). It was seen from the investigation of DCA in dependence of rest time that charge acceptance decreases by about 20% already within the first hour of rest time. (The next 20% DCA are lost within the next 4.5–5 h of rest time. This is not taken up into the test procedure as it would tremendously prolong the duration of the MCT.)

In step 10 the 'vehicle' is cranked again. The following micro-cycling block is supposed to simulate a driving phase at pSoC operation and includes 'boost' charging (step 12) with positive charge balance. Regenerative braking is twice as long as compared in step 8 and 'power net' basic load is reduced (step 11 compared to step 7). Furthermore, the micro-cycling block takes eight times longer than the block with negative charge balance. Of course, effective charge balance is again determined by battery DCA. If DCA was sufficient to accept 50 A during 20 s, DoD is positive with +10.3%. However, if the average charge acceptance during step 12 falls below 16 A, also the 47-fold block turns into negative charge balance. Step 13 states another 1 h break. The following 6-fold micro-cycle block in steps 15 and 16 corresponds to steps 7 and 8 (DoD ∼ −3.7% best case).

Steps 5–16 form one cycle iteration, which is repeated 50 times. As indicated by the vertical dashed line in Fig. 1 the SoC is the critical monitored parameter of the test. If battery DCA is maximum, the charge balance is positive for the first cycle iteration and SoC may increase to 82.4% (just by simple current integration and independent of the charge factor). If a charge factor (CF) of 1.1 would be

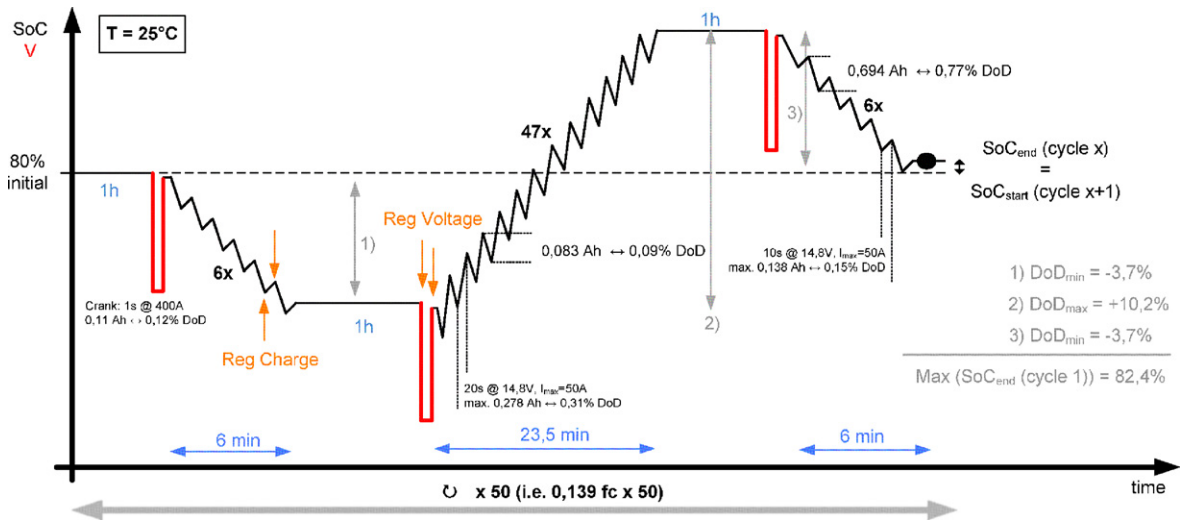

Fig. 1. Graphical overview of the micro-cycling test proposal. Within one cycle iteration (from left to right) there are three micro-cycle blocks (2 blocks, 6-fold and 1 block, 47-fold) with rest times and high-rate loads in between. Fifty cycle iterations are repeated forming one unit. According to an initial specification proposal ten units have to be passed.

arithmetically considered, the corresponding charge balance would still be positive and the SoC would account for 80.9%; the test was intentionally parameterised this way. The SoC after one cycle iteration is the initial SoC for the next iteration. The main idea of the test is monitoring the SoC versus cycle iterations since a trade-off is included in the test. An increase of SoC in the cycle iterations is opposed by a decreased DCA due to lower effective charge potential during 'boost' charging (steps 8, 12, 16). A decrease of SoC over the cycle units is opposed by increased DCA due to enhanced effective charge potential. After fifty cycle iterations the actual battery capacity C_{act} is measured with reference to the initial capacity before the test (steps 1, 20). Then, battery SoC is adjusted to 80%·C_{act} and the next fifty cycle iterations are performed. Fifty cycle iterations are termed as a cycle unit in the following. One unit accounts for about 7 full cycles (fc) for a 90 Ah battery. The figures shown in the next section depict the SoC at the beginning of each cycle iteration, i.e. there are fifty data points per unit. For reasons of simplicity and comparability the SoC is determined on the basis of CF = 1. This kind of data presentation does not influence the qualitative insights of the test.

3. Results

Several batteries from different manufacturers and of different designs were tested with the presented procedure. The suppliers are anonymised by numbers. These numbers correspond to the numbers already assigned in Refs. [1,6,7].

In Fig. 2 the development of the SoC level as described in the previous section is given for battery types #1 and #3 (up-to-date 90 Ah VRLA-AGM) indicated by framed square symbols. It is seen from the first cycle iterations in the first unit that the SoC increases from cycle iteration to cycle iteration up to 87–88%. In line with the discussion of charge balance given above, the SoC increase was intended by the test parameters. However, after the first ten iterations a local SoC maximum is reached and the SoC decreases. The turning point occurs most probable due to the 1 h break in steps 5, 9, 13 and the lower effective charge potential. The negative SoC gradient, which sets in, continues to the end of the cycle block. It is observed that the decreasing SoC is not compensated by the increasing effective charge potential. This is seen from battery DCA in step 12 in Table 1 and Fig. 1. For each of the fifty cycle iterations battery DCA is measured two times. The first value presents the

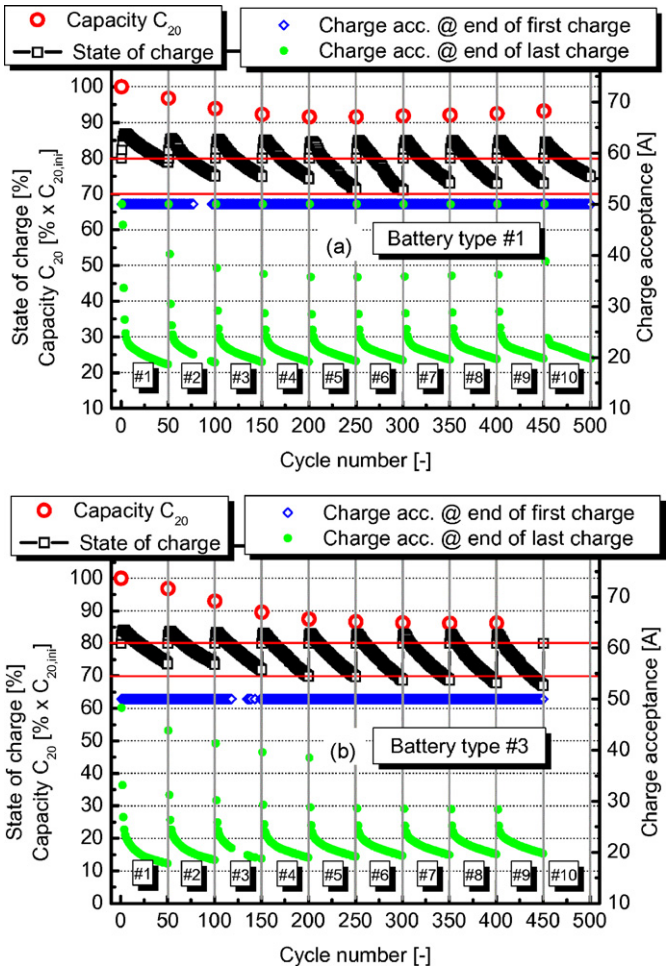

Fig. 2. The micro-cycling test was performed for VRLA-AGM batteries (90 Ah) from several suppliers and manufacturers. The same anonymised nomenclature for the different battery designs is applied like in Refs. [1,6,7]. The SoC is given by the square symbols. It is observed that a local maximum of the SoC is reached within each unit. In the following the SoC decreases approximately linearly as does the DCA (full circle symbols). This refers to the end of the last charging in the 47-fold block in Table 1 (step 12). Battery type #1 passes the test, battery type #3 is just below the limit after unit 6.

current at t_{charge} = 20 s in step 12 for the first of the 47 micro cycles (rhombic-framed symbols) and for the last of the micro cycles in the 47-fold micro-cycle block (full circle symbols). It is observed that the first 'boost' charging is at its maximum (50 A) for the entire cycle unit. This is not surprising as it always follows the high-rate load of step 10. However, the last 'boost' charging degrades tremendously and turns into a linear gradient. It has to be noted that the decrease continues also in the range where the SoC decreases as well. This means that the increasing effective charge potential due to shrinking SoC does not result in improved DCA, but in an even further decreasing DCA.

After a cycle unit the battery is tested for its C_{20} (framed circles and step 20 in Table 1). It is observed for battery type #1 that 10% of the initial capacity is lost after 4–5 cycle blocks, i.e. after about 28–35 fc. Then, a C_{20} minimum is reached and the capacity increases again. This behaviour is partially supported by the test procedure as the SoC at the beginning of each cycle unit is adjusted to 80% of the latest C_{20}. Thus, the absolute amount of charged active mass decreases from unit to unit if the C_{20} values decrease. Of course, this effect promotes the effective charge potential. Surprisingly, the decrease of the C_{20} value is not only stopped and kept constant for a few cycle blocks by this effect, but the C_{20} increases again close to 95% of the initial value after 10 blocks, i.e. 70 fc. A slight increase is also observed in case of battery type #3. A kind of recovery is observed for battery DCA, too. This is seen from the charge current of the last boost charging in the 47-fold micro-cycle block. The second and the third value in each unit also show a local minimum in units 4 and 5.

The presented test covers critical aspects for applying LA batteries in the MHPS. The batteries have to get along with operation at pSoC and battery DCA is the key parameter for the course of the test. In the first attempt the test was specified as 'passed' if the SoC remains above 70% for ten units. This corresponds to about 70 fc and to a test duration of around 17 weeks. Thus, the duration is comparable to that of the 17.5% DoD test (18 weeks), which is usually part of VRLA-AGM battery homologation.

The second criterion for passing the test is the voltage minimum at the end of the warm cranks (step 6, 10, 14). It was shown in Ref. [1] that in terms of ASSF the internal resistance is a key parameter for reasons of power net stability. The minimum voltage during cranking must not drop below 9 V for ten units, i.e. 1500 warm cranks. In Fig. 3a) the voltage is given at the end of the steps 6, 10, 14 and the internal resistance with reference to the OCV after the 1 h break before the crank (Fig. 3b). Because of technical problems with the data acquisition system, the data are not shown after the fifth unit. However, the main message is not affected. The observation regarding scattering of the internal resistance as given in Ref. [1] is confirmed once again. At the beginning of cycling (unit 1) the minimum voltage follows a continuous characteristic. However, the internal resistance is much more affected by scattering than e.g. DCA. Already in the second block large scattering sets in so that the warm cranks, which take place at different SoCs, are not distinguishable anymore and form a decreasing 'data cloud'. As described in Ref. [1] this makes durability prediction and verification of the batteries regarding automatic start and stop systems very difficult. The indicated linear fit with extrapolation in Fig. 3a) shows that about 150 mV additional voltage drop occurs per unit (+0.3 mΩ per unit). As a result, battery type #1 would pass also the second criterion if the assumption of linear extrapolation is correct.

Battery type #1 out of Figs. 1a and 3 was torn down after the test (see Fig. 4). No special findings can be reported of the negative electrode. Only slight surface sulphation across the entire plate was detected and little plate stratification was measured by titration analysis. About 7.5 mass-% of $PbSO_4$ content in the negative active mass was measured across reference plates of the same type before the test; after the test 7.3 mass-% were measured at the top and 11.3 mass-% were measured at the bottom of negative randomly selected electrodes of battery type #1. At the positive electrode moderate corrosion was observed (Fig. 4a). The manual corrosion test was complemented by grid polishing and optical microscopy (b). Based on field operational tests it has already been reported in Refs. [7,9] that pSoC operation barely affected the negative electrode of VRLA-AGM batteries. Instead, corrosion of the positive grid and adhesion of the positive active mass were identified as the main degradation mechanisms. Thus, the investigations done so far indicate that the given test proposal reflects pSoC operation not only in theory, but is in congruence to real-life experience according to the current state of knowledge. Of course, this has to be further confirmed.

However, so far there have been no reports about an accelerated test procedure for the typical load profile in the MHPS with approved transferability to the field. Various approaches for such test procedures have been discussed in the global battery community for a few years. The most prominent example aims at high frequency of high-rate loads in automatic start/stop application. This is the SBA S 0101 idling stop pattern life test developed for flooded batteries of the Battery Association of Japan [10,11,12]. It has been found that especially the negative plate lugs of flooded batteries suffer from corrosion [11].

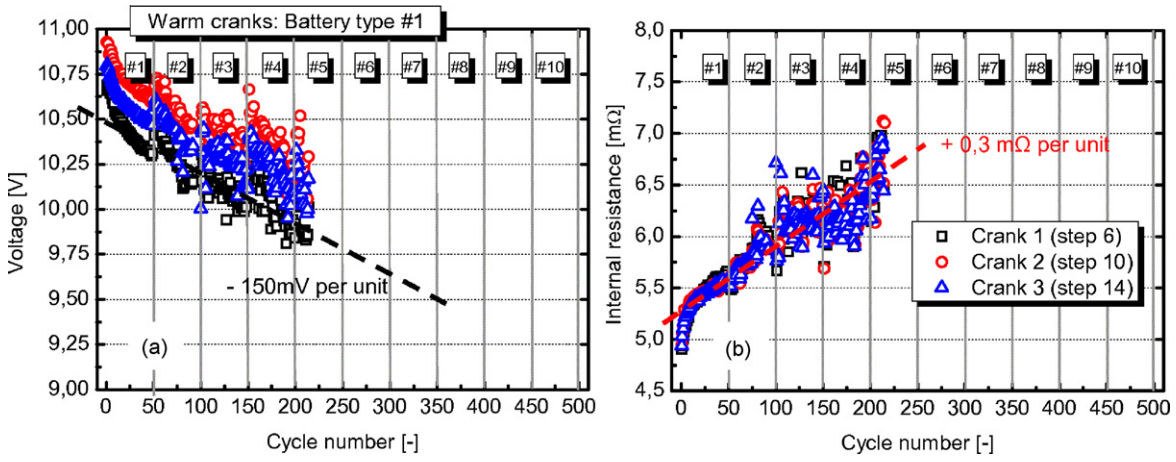

Fig. 3. The minimum voltage and the internal resistance were measured for battery type #1 according to the warm cranks in steps 6, 10 and 14 in Table 1. Data after unit 5 are not depicted due to technical problems with the data acquisition system. The internal resistance increases with +0.3 mΩ per unit and is accompanied by 150 mV decrease per unit. The high scattering of the parameter R_i has to be noted. This makes lifetime predictions concerning start/stop systems quite challenging.

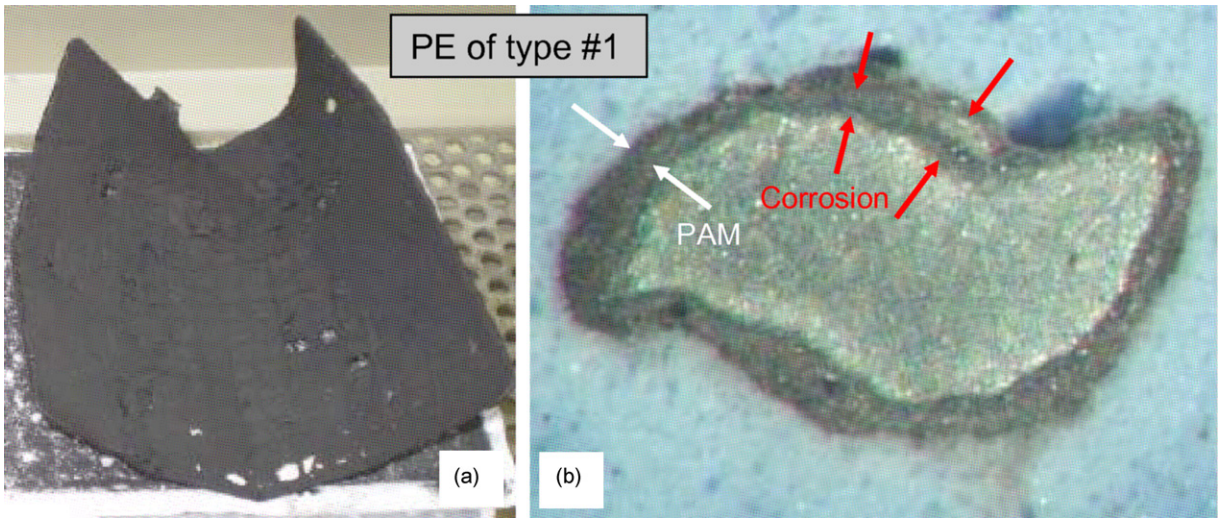

Fig. 4. TDA of battery type #1 (Figs. 2 and 3) after the micro-cycling test. The positive electrode showed moderate corrosion in manual testing (a), which was confirmed by optical microscopy of an intersectional grid polish (b).

Flooded batteries were also subject to the presented test proposal. Both conventional flooded batteries (battery manufacturer #1) and a first generation of so-called 'enhanced' or 'advanced' flooded batteries (sample battery by manufacturer #4) were measured. For proprietary reasons the design details of the enhanced flooded battery cannot be reported. Anyway, flooded batteries – if enhanced (Fig. 5a) or conventional (Fig. 5b) – fail the test in the first unit. At the end of the first unit DCA is considerably below 15 A whereas VRLA-AGM batteries (battery type #1 and type #3) maintain at least 20 A for several units. It is assumed that flooded types rapidly suffer from acid stratification. This weakens the effective charge potential due to increased acid density by locally increased potential at the bottom of the plates. Thus, the difference of the absolute values of charge currents and discharge currents during the test continuously increases, which also promotes stratification since different plate regions are affected by the electrochemical reactions in the vertical direction. The electrolyte concentration of the flooded batteries was not directly measured experimentally after the test, so that the explanatory approach of acid stratification is verified indirectly: The open circuit voltage was measured after step 3 in Table 1 for all batteries. For the flooded batteries it was observed after each unit that this voltage exceeded the voltage of the VRLA-AGM batteries by 0.3–0.5 V, which is clearly a sign of locally increased potentials. Furthermore, as reported above, the TDA of the VRLA-AGM batteries revealed slight stratification of the negative active mass, which allows the conclusion that stratification phenomena are to be expected in the flooded batteries as well.

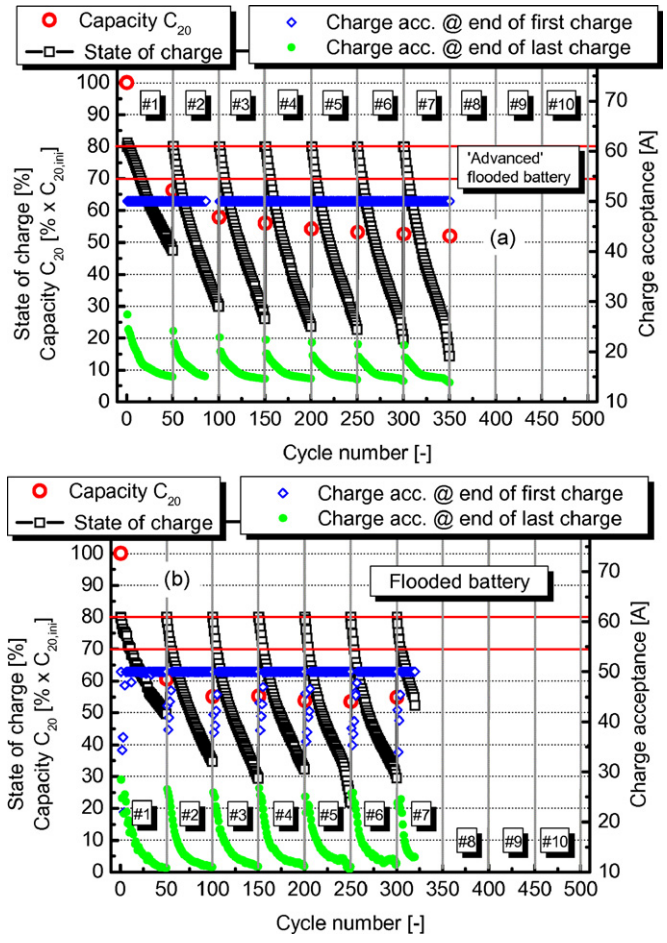

Fig. 5. Flooded batteries were not successful in the micro-cycling test. Both the 'advanced' or 'enhanced' flooded battery (a) and the standard flooded battery (b) (90 Ah) failed already in the first unit. Very likely acid stratification is the main root cause. DCA rapidly drops below the level of VRLA-AGM batteries (compare Fig. 2).

About 40% of initial capacity is lost by the flooded batteries after two units, i.e. less than 15 fc. This result underlines that flooded batteries are not suited for application in MHPS vehicles as stated also in Ref. [8].

4. Summary and discussion

A test proposal for LA battery operation in the MHPS was presented. The test covers especially battery DCA and internal resistance. A first specification (taking 17 weeks of testing) was given, which may be passed by state-of-the-art VRLA-AGM batteries with a narrow margin. Thus, selectivity of the test was proven. Especially flooded batteries do clearly fail the test. Under the operational conditions simulated in the MCT it can be concluded that flooded batteries are not as suitable for application in micro-hybrid electric vehicles as VRLA-AGM batteries. It was also shown that DCA is at least by a factor of two worse as compared to VRLA-AGM batteries – within a few full cycles. These results are confirmed by long-term bench tests [6] and field operational tests [7,8].

Like any accelerated test, the presented test proposal does not reflect real-time conditions. For example, the C_{20} measurement,

which is performed after each cycle unit, is accomplished for monitoring the actual battery capacity. Of course, there is no equivalent to that in customer operation. Furthermore, it is reported in Ref. [6] that the C_{20} measurement has significant (positive) influence on the further operational behaviour of a LA battery at pSoC. As this measurement is performed every ~7 fc, the battery refresh function as introduced in Refs. [6,8] is skipped in the test. This is because the rhythm is comparable to the duty cycle of the battery refresh function (fully charging the battery on a regular base for prevention of hard sulphation of the negative active mass). Thus, the refresh was substituted by the C_{20} test in order to acquire more information during testing.

Acknowledgement

We gratefully thank H. Koch (Combatec GmbH) for constructive cooperation in the TDA.

References

[1] S. Schaeck, A.O. Stoermer, F. Kaiser, L. Koehler, J. Albers, H. Kabza, J. Power Sources 196 (2011) 1541–1554.
[2] DIN EN 50342-1, Lead-acid starter batteries – General requirements and methods of test, November 2006.
[3] H.A. Kiehne (Ed.), Batterien: Grundlagen und Theorie, aktueller technischer Stand und Entwicklungstendenzen, Expert Verlag, Renningen, 1980.
[4] BMW Group, Wartungsfreie PKW-Starterbatterien (Anforderungen, Prüfungen), 2000.
[5] J. Albers, E. Meißner, S. Shirazi, Presented at 12th European Lead Battery Conference (12ELBC), Istanbul, 21–24 September, J. Power Sources, (2010), submitted for publication.
[6] S. Schaeck, A.O. Stoermer, E. Hockgeiger, J. Power Sources 190 (2009) 173–183.
[7] S. Schaeck, T. Karspeck, C. Ott, D. Weirather-Koestner, A.O. Stoermer, J. Power Sources (2010), in press, doi:10.1016/j.jpowsour.2010.08.101.
[8] S. Schaeck, T. Karspeck, C. Ott, M. Weckler, A.O. Stoermer, J. Power Sources, accepted manuscript.
[9] K. Sawai, T. Ohmae, H. Suwaki, M. Shiomi, S. Osumi, J. Power Sources 174 (2007) 54–60.
[10] Battery Association of Japan. Start-up lead-acid battery for idling-stop cars. Test method, performance, dimensions and marking. Standard SBA A0101, 2005.
[11] T. Takeuchi, K. Sawai, Y. Tsuboi, M. Shiota, A. Ishimoto, N. Hirai, S. Osumi, J. Power Sources 189 (2009) 1190–1198.
[12] T. Kondo, T. Takeuchi, M. Shiomi, K. Sawai, Y. Tsuboi, M. Shiota, S. Ishimoto, Proceedings of the 1st Technical Conference "Advanced Battery Technologies for Automobiles and Their Electric Power Grid Integration", Essen, Germany, January 20–21, 2009.